



**HAL**  
open science

## Selective Reductive Dimerization of CO<sub>2</sub> into Glycolaldehyde

Dan Zhang, Carlos Jarava-Barrera, Sébastien Bontemps

► **To cite this version:**

Dan Zhang, Carlos Jarava-Barrera, Sébastien Bontemps. Selective Reductive Dimerization of CO<sub>2</sub> into Glycolaldehyde. ACS Catalysis, 2021, 11 (8), pp.4568-4575. 10.1021/acscatal.1c00412. hal-03231103

**HAL Id: hal-03231103**

**<https://hal.science/hal-03231103v1>**

Submitted on 20 May 2021

**HAL** is a multi-disciplinary open access archive for the deposit and dissemination of scientific research documents, whether they are published or not. The documents may come from teaching and research institutions in France or abroad, or from public or private research centers.

L'archive ouverte pluridisciplinaire **HAL**, est destinée au dépôt et à la diffusion de documents scientifiques de niveau recherche, publiés ou non, émanant des établissements d'enseignement et de recherche français ou étrangers, des laboratoires publics ou privés.

# Selective reductive dimerization of CO<sub>2</sub> into glycolaldehyde

*Dan Zhang, Carlos Jarava-Barrera, Sébastien Bontemps\**

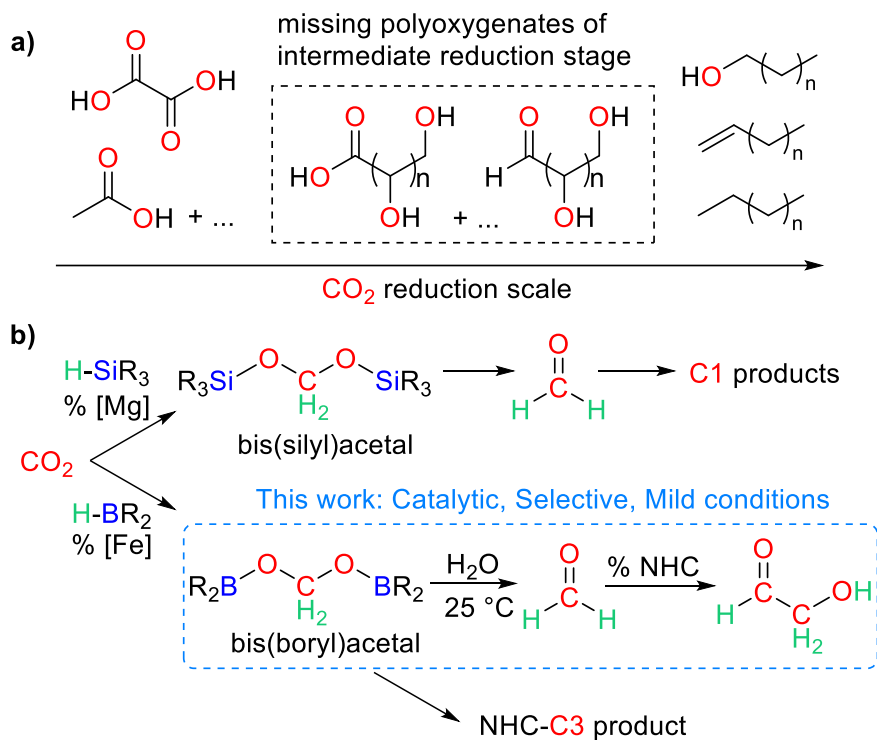
LCC-CNRS, Université de Toulouse, CNRS, 205 route de Narbonne, 31077 Toulouse Cedex 04, France.

Keywords: CO<sub>2</sub> reduction, Organo-catalysis, Formose reaction, Dimerization, Carbohydrates

The selective dimerization of CO<sub>2</sub> into glycolaldehyde is achieved in a one-pot two-step process via formaldehyde as a key intermediate. The first step concerns the iron-catalyzed selective reduction of CO<sub>2</sub> into formaldehyde via formation and controlled hydrolysis of a bis(boryl)acetal compound. The second step concerns the carbene-catalyzed C-C bond formation to afford glycolaldehyde. Both carbon atoms of glycolaldehyde arise from CO<sub>2</sub> as proven by labelling experiment with <sup>13</sup>CO<sub>2</sub>. This hybrid organometallic/organic catalytic system employs mild conditions (1 atm of CO<sub>2</sub>, 25 °C to 80 °C in less than 3 h) and low catalytic loadings (1 % and 2.5%, respectively). Glycolaldehyde is obtained in 53% overall yield. The appealing reactivity of glycolaldehyde is exemplified i) in a dimerization process leading to C<sub>4</sub> aldose compounds and ii) in a tri-component Petasis-Borono-Mannich reaction generating C-N and C-C bond in one process.

## INTRODUCTION

CO<sub>2</sub> reductions to C<sub>n>1</sub> products are much less developed than to C<sub>1</sub> compounds, due to the intrinsic difficulty of combining two individually challenging steps in a single process: CO<sub>2</sub> reduction and C-C bond formation.<sup>1</sup> As a consequence, further developments of CO<sub>2</sub> utilization as C<sub>n</sub> source face two main issues: selectivity and limited scope of products.<sup>1-2</sup> Besides oxalate, acetate and related products,<sup>3</sup> most of the obtained compounds are highly reduced products: aliphatic hydrocarbons, olefins and alcohols (Scheme 1a). In these electroreduction or hydrogenation systems, CO is considered as the key bifurcation point toward C<sub>n</sub> products. Because of their high energy density, the synthesized products are of interest as energy carriers. However, if one wants to use CO<sub>2</sub> as a sustainable C<sub>n</sub> source, less reduced polyoxygenated compounds would be highly desirable (Scheme 1a), because such compounds, featuring multiple alcohol, ketone and/or aldehydic functions, exhibit appealing molecular complexity leading to versatile reactivity. Their isolation from biomass is currently being explored for their use as new chemical feedstock.<sup>4</sup> Finding a new access from CO<sub>2</sub>, would offer a complementary sustainable alternative to biomass extraction. A thorough study on Cu-catalyzed electroreduction of CO<sub>2</sub> reported the detection of such C<sub>2</sub> and C<sub>3</sub> oxygenated compounds as minor species.<sup>5</sup> As indicated in the proposed mechanism and further complemented by an in-depth theoretical investigation,<sup>6</sup> these compounds cannot be accumulated because they are further reduced *in situ* (Scheme 1a) under the reaction conditions.



**Scheme 1.** a)  $\text{C}_n$  products obtained from electroreduction and hydrogenation of  $\text{CO}_2$ ; b) Synthesis and utilization of  $4e^-$  reduction products as C1 source from  $\text{CO}_2$  hydrosilylation<sup>7</sup> and as  $\text{C}_n$  source from  $\text{CO}_2$  hydroboration.<sup>8</sup>

We believe that i) new pathways need to be developed for the generation and accumulation of these reactive intermediates, ii) homogeneous thermal transformations of  $\text{CO}_2$  into  $\text{C}_n$  compounds would have a key role to play in this objective<sup>9</sup> and iii)  $\text{HCHO}$  could be an alternative bifurcation point toward  $\text{C}_n$  products. Mild operating conditions should be pursued to favor in situ characterization and control of the reaction. In the field of  $\text{CO}_2$  reduction, hydrosilane and hydroborane reductants enabled to use particularly mild conditions and make significant progress in mechanisms understanding as well as in the characterization and functionalization of reactive intermediates.<sup>10</sup> More specifically, it enabled the development of reduction of  $\text{CO}_2$  to the formaldehyde level with the selective generation of bis(silyl)<sup>11</sup> and bis(boryl)acetal<sup>12</sup> compounds

(scheme 1b). These reactive intermediates were proven particularly versatile for the synthesis of a large scope of different C<sub>1</sub> products.<sup>8, 11c, 12d, 12f, 13</sup> While these acetal compounds were used as formaldehyde surrogates, it is only in a recent example, that Parkin et al. reported the actual release of formaldehyde from a bis(silyl)acetal compound by adding CsF at 25 °C or heating the solution to 120 °C in DMF.<sup>7</sup> The in situ generated formaldehyde was then involved in C<sub>1</sub> transformations (Scheme 1b).

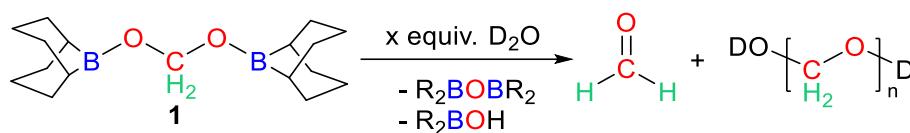
In the last 10 years, we developed 4e<sup>-</sup> reductions of CO<sub>2</sub> with hydroboranes<sup>14</sup> and applied it to C<sub>1</sub> chemistry.<sup>12f, 15</sup> More recently, we aimed at using this process for the transformation of CO<sub>2</sub> into C<sub>n</sub> products. A first example of the synthesis of a C<sub>3</sub> compound was reported from the stoichiometric reaction of an N-Heterocyclic Carbene (NHC) with a bis(boryl)acetal compound.<sup>8</sup> However, the coupling step was not catalytic and the yield (30%) remained modest. Herein, we present the first catalytic system enabling to generate selectively glycolaldehyde from the CO<sub>2</sub> reductive dimerisation in 62% yield from a bis(boryl)acetal compound.

## RESULTS AND DISCUSSION

### Step 1: Formaldehyde release from bis(boryl)acetal

As reported earlier, bis(boryl)acetal **1** is generated from the selective 4e<sup>-</sup> reduction of CO<sub>2</sub> with 9-BBN using mild conditions (25°C, 1 atm of CO<sub>2</sub>, 45 min.) and 1 mol% of the iron complex Fe(H)<sub>2</sub>(dmpe)<sub>2</sub> (Scheme 2).<sup>12f</sup> The first objective was to find a pathway to generate formaldehyde from bis(boryl)acetal **1** under mild and compatible conditions for the subsequent organo-catalyzed coupling step (vide infra). While partial release of HCHO was mentioned in the literature from a bis(boryl)acetal featuring pinacolboryl moieties,<sup>12d, 14b, 16</sup> no system actually reported quantitative generation of HCHO from bis(boryl)acetal compound as in Parkin's example from a related bis(silyl)acetal.<sup>7</sup> In this context, compound **1** was subjected to 1, 2 and 10 equivalents of water

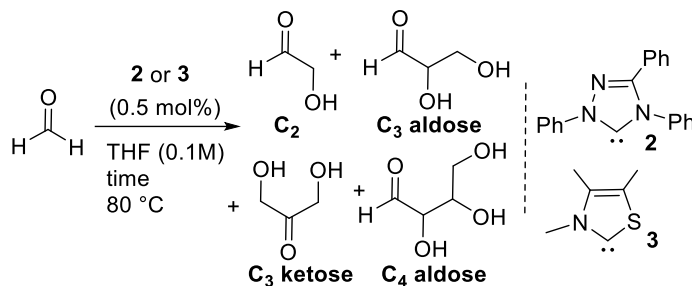
(Scheme 2). While 1 and 2 equiv. led to partial release of formaldehyde in 24 and 72% yield, respectively (even after 24 h), the use of 10 equiv. afforded formaldehyde in 94% yield within 30 min. Formaldehyde was detected by  $^1\text{H}$  NMR analysis both as free formaldehyde (singlet at 9.58 ppm) and as hydrated or oligomeric formaldehyde (broad signals at 4.5-5.5 ppm). Both sets of resonances were measured against an internal standard to calculate the yield in formaldehyde (see Table S2 and Figure S1 in ESI for details).



**Scheme 2:** Step 1: Release of HCHO from reactivity of **1** with  $\text{D}_2\text{O}$ .

### Step 2: Carbene-catalyzed formose reaction of HCHO in the presence of water

We then turned our attention to the formation of short chain carbohydrates from HCHO. The so-called formose reaction corresponds to the oligomerization of formaldehyde into carbohydrate compounds. While this powerful transformation<sup>17</sup> was discovered in the 19th century,<sup>17</sup> it suffers from numerous side reactions leading to mixtures of up to 30 different products when catalyzed by inorganic bases.<sup>18</sup> Net improvements in controlling side reactions and chain growth were achieved with the use of NHC-type catalysts, notably with thiazolium and triazolium precursors.<sup>18-19</sup> In these studies, it is clear that formose outcome is very sensitive to the reaction conditions (solvent, NHC, reaction time), however i) beyond the accepted general mechanism via Breslow intermediate, more defined rationales to explain such variations are lacking<sup>19c-e</sup> and ii) THF and  $\text{H}_2\text{O}$  are two solvents that have been sparingly used.<sup>19e, 20</sup>

**Table 1.** Step 2: Formose reaction in DMF, THF and THF/H<sub>2</sub>O media with catalyst **2** and **3**.<sup>a</sup>

Entry	Time min	NHC	Solvent	C <sub>2</sub> <sup>b</sup> %	C <sub>3</sub> <sup>b</sup> %	C <sub>4</sub> <sup>b</sup> %	Total yield %
1	10	2	DMF	33	-	-	33
2	30	2	DMF	62	34	-	96
3	60	2	DMF	38	28	34	100
4	10	2	THF	16	-	-	16
5	30	2	THF	16	-	72	88
6	60	2	THF	17	5	78	100
7	30	2	THF+H <sub>2</sub> O <sup>c</sup>	27	18	11	56
8	30	2	THF+H <sub>2</sub> O <sup>d</sup>	31	-	-	31
9	30	2	THF+H <sub>2</sub> O <sup>e</sup>	17	-	-	17
10	30	2	THF+MeOH <sup>f</sup>	37	3	-	40
11	30	3	THF	12	67	4	93
12	30	3	THF+H <sub>2</sub> O <sup>c</sup>	-	-	-	0

<sup>a</sup> Reaction conditions: 0.5 mmol of paraformaldehyde, 0.0025 mmol of carbene, 5 mL of THF (0.1 M), 80 °C. <sup>b</sup> GC yields obtained after derivatization reactions. <sup>c</sup> 10 equiv. of water were added relative to HCHO amount. <sup>d</sup> 20 equiv. of water were added relative to HCHO amount. <sup>e</sup> 40 equiv. of water were added relative to HCHO amount. <sup>f</sup> 1 equiv. of MeOH was added relative to HCHO amount.

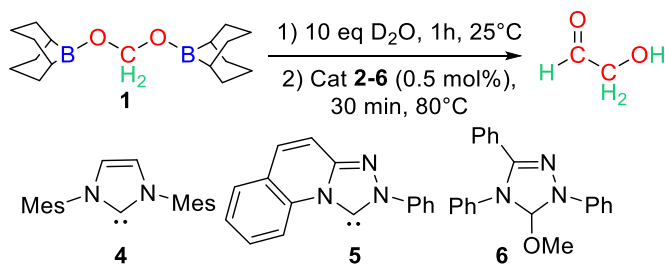
In this context, NHC **2** and **3** were selected for initial tests with commercial para-formaldehyde in DMF, THF and THF/H<sub>2</sub>O media (Table 1). Results reported by Teles et al. in DMF were first

reproduced with catalyst **2**, showing that 30 and 60 min were necessary to reach full conversion. Glycolaldehyde (C<sub>2</sub>) was the main product after 30 min while a mixture of C<sub>2-4</sub> carbohydrates was observed after 60 min with 0.5 mol% catalyst loading (Table 1, entries 1-3).<sup>19e</sup> Two formose reactions were reported in THF with triazolium precursors, slightly different from **2**, leading to the favored formation of glycolaldehyde in 62% and 46% yields.<sup>19e, 19f</sup> We thus explored the reaction in THF with catalysts **2** and **3**. The reaction was almost complete after 30 min: 88% and 93% total yield with **2** and **3**, respectively (Table 1, entries 5 and 11). Interestingly, **3** favored the dihydroxyacetone (C<sub>3</sub> ketose) with a measured 67% yield after 30 min, and **2** favored the C<sub>4</sub> aldoses (erythrose and threose) with combined yields of 72% and 78% after 30 and 60 min, respectively. C<sub>4</sub> ketoses were never detected. To the best of our knowledge, these latter results are the best yields and selectivity reported for C<sub>4</sub> aldoses. Teles et al. indeed reported two reactions in DMF in which the C<sub>4</sub> carbohydrates were the major products with yields of 50% and 16% with triazolium and imidazolium precursors as catalyst, respectively.<sup>19e, 19f</sup> We then probed the impact of the addition of H<sub>2</sub>O which was reported detrimental for the reaction yield and the selectivity in DMF/H<sub>2</sub>O thiamine-based catalysis.<sup>20</sup> In accordance with these data, we observed a general negative impact of H<sub>2</sub>O on the yield. However, while the addition of 10 equiv. of water completely shut down any conversion with catalyst **3** (Table 1, entry 12), we were pleased to observe a 56% total yield of C<sub>2-4</sub> aldose products with catalyst **2** after 30 min in the same conditions. The addition of 20 and 40 equiv. of water or 1 equiv. of methanol afforded lower total yields (Table 1, entries 8-10). With these positive results from HCHO in presence of water in hands, we then decided to explore this transformation from CO<sub>2</sub>.

### **Synthesis of glycolaldehyde from CO<sub>2</sub>**



We combined the two reactions developed above in a one-pot system. The conditions deduced from these independent studies are as follow: bis(boryl)acetal **1** generated *in situ* in THF was hydrolyzed with 10 equiv. of water at 25°C in 1 h. 0.5% of NHC **2** was then added to catalyze the formose reaction at 80 °C in 30 min (Scheme 3). To our delight, glycolaldehyde was generated in 37% yield under these standard conditions. The yield is the average yield of 4 runs with a measured maximum deviation ( $\Delta_{\max}$ ) of 7%. **C3** and **C4** carbohydrates were detected in 0.4 and 0.6% yield, respectively. The reaction was thus particularly selective since no other carbohydrate was detected, although the yield remained modest. The reaction took place only in the presence of carbene catalyst **2** or its triazolium precursor **6**. Their absence or the use of carbenes **3-5** did not afford any detectable **C2**, **C3** or **C4** products.<sup>21</sup> Future work will be dedicated to understand the specificity of carbene **2** in protic media, keeping in mind recent questioning about organo-catalyzed umpolung reactions.<sup>22</sup>



**Scheme 3.** One-pot system under initial standard conditions with catalyst **2-6**.

In order to improve glycolaldehyde yield, reaction conditions were optimized using catalyst **2**. The optimization was conducted in two stages: i) variation of one parameter at a time (Scheme 4a), and ii) combination of optimal conditions and careful comparison of the obtained yields between standard (s) and optimized (o) conditions (Scheme 4b).

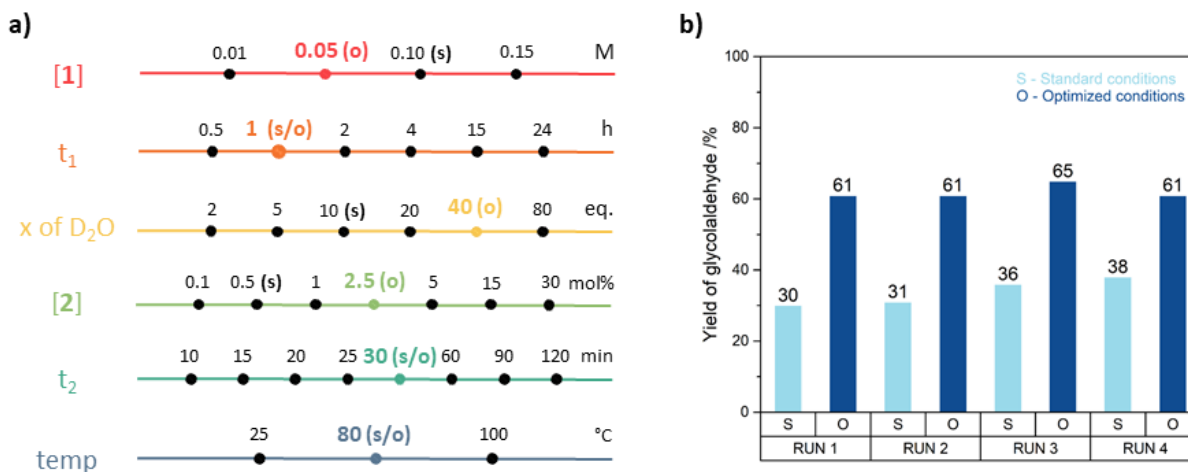
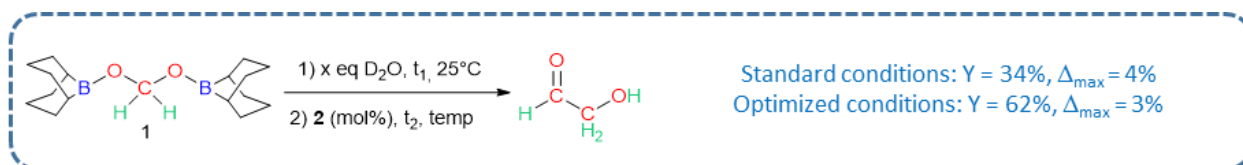
*First stage* (Scheme 4a): 6 parameters were optimized: the initial concentration of compound **1** in THF, the time  $t_1$  of the hydrolysis, the number of equivalents of  $D_2O$  added for hydrolysis, the

catalyst loading in **2**, the time ( $t_2$ ) and temperature (temp) of formose reaction. For each parameter, standard (s) and determined optimal (o) condition are indicated among the different conditions tested (in black color). Details on observed trends for each parameter are described hereafter in the order indicated in Scheme 4a while detailed yields are given in ESI. A significant yield improvement of about 10% was observed when the initial concentration of **1** in THF was divided by half ( $[1] = 0.05$  M). This observed trend is consistent with the common observation of lower chain length selectivity with lower concentration of formaldehyde in formose reaction.<sup>19b, 19c, 19e</sup>

The hydrolysis time of the acetal **1** ( $t_1$ ) had a negligible impact on the yield when it was varied from 30 min to 24 h. It indicates that compound **1** is readily hydrolyzed in these conditions. However, we observed improved yields in glycolaldehyde when 40 equiv. of water were used instead of 2, 5, 10, 20 or 80. Since the hydrolysis of the acetal **1** ( $t_1$ ) had no impact on the yield, we believe that the increased yield with 40 equiv. of H<sub>2</sub>O was not due to a better hydrolysis process but rather to a dilution factor. Adding 40 equiv. of H<sub>2</sub>O indeed led to a decrease of the concentration by about half which was shown to be beneficial above. We confirmed this assumption by varying the amount of equiv. of H<sub>2</sub>O added while maintaining  $[1]$ . In this case, yield improvement was attenuated, but still in favor of the addition of 40 equiv. of H<sub>2</sub>O. Although the observed +4% increase is marginal, we kept 40 equiv. of H<sub>2</sub>O as an optimized condition, while maintaining concentration  $[1] = 0.05$  M. When catalyst loading  $[2]$  was varied from 0.1 to 30 mol%, a narrow variation of 10% was observed between the highest and the lowest yields. 2.5 mol% catalyst loading was found optimal. It first indicates that the catalyst is very active under these conditions. It also shows that if H<sub>2</sub>O has a detrimental impact, its excess compared to the amount of catalyst (3 to 4 orders of magnitude) is too large to be compensated by a 10-fold increase of the catalyst loading. Finally, the standard conditions for formose reaction time and temperature

( $t_2 = 30$  min, temp = 80 °C) are also the optimal conditions, in accordance with the literature.  $t_2 = 25$  or 30 min enabled to record the best yields, while shorter or longer reaction time had a negative impact. We confirmed that the reaction took place at 100°C but with a slightly lower yield, while expectedly, it did not proceed at room temperature.

*Second stage* (Scheme 4b): The presented general optimization methodology relies on a classical one-factor-at-a-time method. Although this is a classical method, combinations of effect are then not considered.<sup>23</sup> In order to properly assess the impact of the optimized conditions, the given yields are the average of 4 runs. In each of them, the solution containing the *in situ* generated **1**, was split into two containers which were then subjected in parallel to the standard conditions (s) for one container and to the optimized conditions (o) for the other one. With these experiments, a 34% yield ( $\Delta_{\max} = 4\%$ ) was measured under the standard conditions, in the same range as that initially obtained (i.e. 37%,  $\Delta_{\max} = 7\%$ ). Gratifyingly, the yield obtained under the optimized conditions is calculated to be 62% with a maximum deviation of 3%. The optimization study thus led to almost doubling the product yield. Considering the system including the CO<sub>2</sub> reduction step, we developed herein a hybrid one-pot organometallic/organic system transforming CO<sub>2</sub> into glycolaldehyde in an overall 53% yield based on hydroborane used, under mild conditions in less than 3h.



**Scheme 4.** Optimization for the synthesis of glycolaldehyde: **a)** one-factor-at-a-time study over 6 parameters, (s) indicates the standard condition, (o) indicates the optimal condition; **b)** comparison of yields between standard and optimized conditions.

### Synthesis of $^{13}\text{C}$ -labeled glycolaldehyde

As a mean to prove that glycolaldehyde is indeed formed from the reductive coupling of two molecules of  $\text{CO}_2$  and to generate valuable  $^{13}\text{C}$ -labeled glycolaldehyde, we conducted the reaction using  $^{13}\text{CO}_2$ . The multiple forms adopted by glycolaldehyde in solution (monomeric, symmetrical and unsymmetrical oligomeric and hydrated forms) complexify its NMR analysis (see ESI).<sup>5, 24</sup> We present herein the characterization of the simple monomeric aldehydic form in the crude THF- $d_8$ / $\text{D}_2\text{O}$  mixture. In  $^{13}\text{C}\{^1\text{H}\}$  NMR analysis, this species is characterized at  $\delta$  203.3 (d,  $^1J_{\text{C-C}} = 41.1$  Hz) and 69.7 (d,  $^1J_{\text{C-C}} = 41.1$  Hz). The two carbon centers correlate with the aldehydic and methylenic protons characterized at  $\delta$  9.60 (dd, 1H,  $^1J_{\text{H-C}} = 173.2$  Hz,  $^3J_{\text{H-C}} = 26.9$  Hz) and 4.01 (dd, 2H,  $^1J_{\text{H-C}} = 140.9$  Hz,  $^3J_{\text{H-C}} = 4.0$  Hz), respectively. Figure 1 discloses the stacking of  $^1\text{H}$  NMR analysis as well as the selective and broad band  $^1\text{H}\{^{13}\text{C}\}$  spectra of the selected areas. It enables

to visualize that each proton correlates with both carbon nuclei of the molecule with observed  $^1J$  and  $^3J$  scalar couplings, the selective  $^{13}\text{C}$  decoupling further highlighting these correlations. Importantly, no  $^{12}\text{C}$ -labeled glycolaldehyde was detected in the crude mixture by  $^1\text{H}$  NMR, indicating that every molecule of glycolaldehyde quantified by GC analyses arises from  $\text{CO}_2$  reductive coupling.

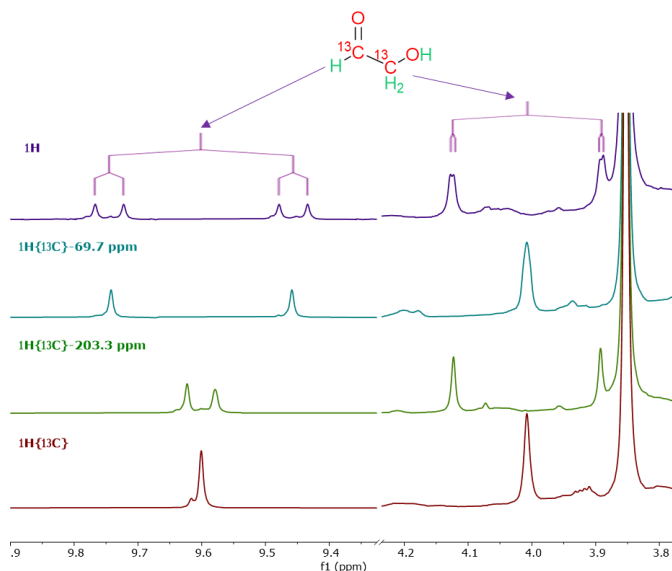
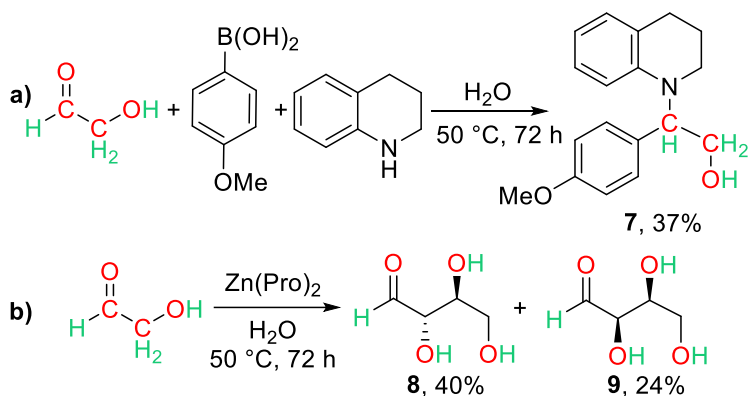


**Figure 1.** Selected areas of  $^1\text{H}$  and  $^1\text{H}\{^{13}\text{C}\}$  NMR analyses of the crude mixture obtained from the developed  $^{13}\text{CO}_2$  reductive coupling process.

### ***In situ* transformation of glycolaldehyde**

Carbohydrates and glycolaldehyde in this instance are attractive species because of their reactive nature.<sup>4e, 25</sup> In order to exemplify this feature, glycolaldehyde *in situ* generated from  $\text{CO}_2$  was engaged in two reactions depicted in Scheme 5a) and b). The tri-component Petasis-Borono-Mannich reaction was conducted in water to afford compound **7**, isolated in 37% yield in aqueous solution.<sup>26</sup> The dimerization of glycolaldehyde was then conducted with  $\text{Zn}(\text{L-Pro})_2$  as catalyst.<sup>27</sup> Increasing the reaction temperature to  $50\text{ }^\circ\text{C}$  enabled to generate erythrose (**8**, 40%) and threose (**9**, 24%) for a total GC yield of 64 % of  $\text{C}_4$  aldoses.



**Scheme 5.** Reactivity of *in situ* generated glycolaldehyde: a) Synthesis of **7** by Petasis Borono-Mannich reaction; b) Synthesis of C<sub>4</sub> carbohydrates.

## CONCLUSIONS

In the present publication, the selective dimerization of CO<sub>2</sub> into glycolaldehyde is reported for the first time. To achieve such transformation, particularly mild conditions (1 atm of CO<sub>2</sub>, 25 °C to 80 °C in < 3 h) and low catalytic loadings (1% and 2.5%, respectively) were employed with a hybrid organometallic/organic catalytic process. Key aspects of the presented work rely on the quantitative release of formaldehyde from the hydrolysis of a bis(boryl)acetal compound compatible with the C-C coupling step. Intensive optimization led to the generation of glycolaldehyde in 62% yield from compound **1** and in 53% overall yield from CO<sub>2</sub> based on the amount of hydroborane engaged. The ultimate proof of CO<sub>2</sub> being the sole source of carbon was obtained with labelling experiment using <sup>13</sup>CO<sub>2</sub>. This homogeneous thermal CO<sub>2</sub> process shows that i) bis(boryl)acetal obtained from mild CO<sub>2</sub> reduction enables a selective and mild access to formaldehyde, ii) acetal compounds can be involved in the generation of C<sub>n</sub> compounds and iii) carbohydrates such as glycolaldehyde are valuable reactive feedstocks to be synthesized from CO<sub>2</sub>.<sup>4e, 25</sup> On a broader perspective, the presented strategy highlights that formaldehyde offers an appealing new synthetic access to C<sub>n</sub> products of intermediate reduction stage. Although, in the present case, the boron-based reductant system is not sustainable and the formose control only

applies to the smallest carbohydrate, we believe that the strategy presented herein could stimulate different fields of CO<sub>2</sub> reduction.

#### AUTHOR INFORMATION

##### **Corresponding Author**

Sébastien Bontemps - LCC-CNRS, Université de Toulouse, CNRS, 205 route de Narbonne, 31077 Toulouse Cedex 04, France; Email: [sebastien.bontemps@lcc-toulouse.fr](mailto:sebastien.bontemps@lcc-toulouse.fr)

##### **Author**

**Dan Zhang** - LCC-CNRS, Université de Toulouse, CNRS, 205 route de Narbonne, 31077 Toulouse Cedex 04, France

**Carlos Jarava-Barrera** - LCC-CNRS, Université de Toulouse, CNRS, 205 route de Narbonne, 31077 Toulouse Cedex 04, France

##### **Author Contributions**

The manuscript was written through contributions of all authors. All authors have given approval to the final version of the manuscript.

#### ASSOCIATED CONTENT

##### **Supporting Information.**

The supporting information are available free of charge. It includes experimental details, compounds synthesis and characterization and description of the optimization procedure.

## ACKNOWLEDGMENT

Chinese Scholarship Council is acknowledged for PhD fellowship of D. Z. The ANR (ICC-ANR-17-CE07-0015) and the CNRS-DR14 are acknowledged for financial and technical support.

## REFERENCES

1. Prieto, G. Carbon Dioxide Hydrogenation into Higher Hydrocarbons and Oxygenates: Thermodynamic and Kinetic Bounds and Progress with Heterogeneous and Homogeneous Catalysis. *ChemSusChem* **2017**, *10*, 1056–1070
2. (a) Todorova, T. K.; Schreiber, M. W.; Fontecave, M. Mechanistic Understanding of CO<sub>2</sub> Reduction Reaction (CO<sub>2</sub>RR) Toward Multicarbon Products by Heterogeneous Copper-Based Catalysts. *ACS Catal.* **2020**, *10*, 1754-1768; (b) Marques Mota, F.; Kim, D. H. From CO<sub>2</sub> methanation to ambitious long-chain hydrocarbons: alternative fuels paving the path to sustainability. *Chem. Soc. Rev.* **2019**, *48*, 205-259; (c) Porosoff, M. D.; Yan, B.; Chen, J. G. Catalytic reduction of CO<sub>2</sub> by H<sub>2</sub> for synthesis of CO, methanol and hydrocarbons: challenges and opportunities. *Energy Environ. Sci.* **2016**, *9*, 62-73; (d) Huan, T. N.; Dalla Corte, D. A.; Lamaison, S.; Karapinar, D.; Lutz, L.; Menguy, N.; Foldyna, M.; Turren-Cruz, S.-H.; Hagfeldt, A.; Bella, F.; Fontecave, M.; Mougél, V. Low-cost high-efficiency system for solar-driven conversion of CO<sub>2</sub> to hydrocarbons. *Proc. Natl. Acad. Sci.* **2019**, *116*, 9735-9740.
3. (a) Banerjee, A.; Kanan, M. W. Carbonate-Promoted Hydrogenation of Carbon Dioxide to Multicarbon Carboxylates. *ACS Cent. Sci.* **2018**, *4*, 606-613; (b) Lan, J.; Liao, T.; Zhang, T.; Chung, L. W. Reaction Mechanism of Cu(I)-Mediated Reductive CO<sub>2</sub> Coupling for the Selective Formation of Oxalate: Cooperative CO<sub>2</sub> Reduction To Give Mixed-Valence Cu<sub>2</sub>(CO<sub>2</sub>•<sup>-</sup>) and Nucleophilic-Like Attack. *Inorg. Chem.* **2017**, *56*, 6809-6819; (c) Liu, Y.; Chen, S.; Quan, X.; Yu, H. Efficient Electrochemical Reduction of Carbon Dioxide to Acetate on Nitrogen-Doped Nanodiamond. *J. Am. Chem. Soc.* **2015**, *137*, 11631–11636; (d) Angamuthu, R.; Byers, P.; Lutz, M.; Spek, A. L.; Bouwman, E. Electrocatalytic CO<sub>2</sub> Conversion to Oxalate by a Copper Complex. *Science* **2010**, *327*, 313-315.
4. (a) Liao, Y.; Koelewijn, S.-F.; Van den Bossche, G.; Van Aelst, J.; Van den Bosch, S.; Renders, T.; Navare, K.; Nicolai, T.; Van Aelst, K.; Maesen, M.; Matsushima, H.; Thevelein, J. M.; Van Acker, K.; Lagrain, B.; Verboekend, D.; Sels, B. F. A sustainable wood biorefinery for low-carbon footprint chemicals production. *Science* **2020**, *367*, 1385-1390; (b) Shylesh, S.; Gokhale, A. A.; Ho, C. R.; Bell, A. T. Novel Strategies for the Production of Fuels, Lubricants, and Chemicals from Biomass. *Acc. Chem. Res.* **2017**, *50*, 2589-2597; (c) Yamaguchi, S.; Baba, T. A Novel Strategy for Biomass Upgrade: Cascade Approach to the Synthesis of Useful Compounds via C-C Bond Formation Using Biomass-Derived Sugars as Carbon Nucleophiles. *Molecules* **2016**, *21*, 937; (d) Corma, A.; Iborra, S.; Velty, A. Chemical Routes for the Transformation of Biomass into Chemicals. *Chem. Rev.* **2007**, *107*, 2411-2502; (e) Faveere, W. H.; Van Praet, S.; Vermeeren, B.; Dumoleijn, K. N. R.; Moonen, K.; Taarning, E.; Sels, B. F. Toward Replacing Ethylene Oxide in a Sustainable World: Glycolaldehyde as a Bio-Based C<sub>2</sub> Platform Molecule. *Angew. Chem. Int. Ed.* **2021**, 10.1002/anie.202009811.
5. Kuhl, K. P.; Cave, E. R.; Abram, D. N.; Jaramillo, T. F. New insights into the electrochemical reduction of carbon dioxide on metallic copper surfaces. *Energy Environ. Sci.* **2012**, *5*, 7050-7059.
6. Garza, A. J.; Bell, A. T.; Head-Gordon, M. Mechanism of CO<sub>2</sub> Reduction at Copper Surfaces: Pathways to C<sub>2</sub> Products. *ACS Catal.* **2018**, *8*, 1490-1499.
7. Rauch, M.; Strater, Z.; Parkin, G. Selective Conversion of Carbon Dioxide to Formaldehyde via a Bis(silyl)acetal: Incorporation of Isotopically Labeled C<sub>1</sub> Moieties Derived from Carbon Dioxide into Organic Molecules. *J. Am. Chem. Soc.* **2019**, *141*, 17754-17762.
8. Béthegnies, A.; Escudí, Y.; Nuñez-Dallos, N.; Vendier, L.; Hurtado, J.; del Rosal, I.; Maron, L.; Bontemps, S. Reductive CO<sub>2</sub> Homocoupling: Synthesis of a Borylated C<sub>3</sub> Carbohydrate. *ChemCatChem* **2019**, *11*, 760-765.
9. (a) Cui, M.; Qian, Q.; He, Z.; Zhang, Z.; Ma, J.; Wu, T.; Yang, G.; Han, B. Bromide promoted hydrogenation of CO<sub>2</sub> to higher alcohols using Ru-Co homogeneous catalyst. *Chem. Sci.* **2016**, *7*, 5200-5205; (b) Tominaga, K.-I.; Sasaki, Y.; Saito, M.; Hagihara, K.; Watanabe, T. Homogeneous Ru□Co bimetallic catalysis in CO<sub>2</sub> hydrogenation: The formation of ethanol. *J. Mol. Catal.* **1994**, *89*, 51-55.



10. (a) Zhang, Y.; Zhang, T.; Das, S. Catalytic transformation of CO<sub>2</sub> into C1 chemicals using hydrosilanes as a reducing agent. *Green Chem.* **2020**, *22*, 1800-1820; (b) Hulla, M.; Dyson, P. J. Pivotal Role of the Basic Character of Organic and Salt Catalysts in C–N Bond Forming Reactions of Amines with CO<sub>2</sub>. *Angew. Chem. Int. Ed.* **2020**, *59*, 1002-1017; (c) P, S.; Mandal, S. K. From CO<sub>2</sub> activation to catalytic reduction: a metal-free approach. *Chem. Sci.* **2020**, *11*, 10571-10593; (d) Fernández-Alvarez, F. J.; Oro, L. A. Homogeneous Catalytic Reduction of CO<sub>2</sub> with Silicon-Hydrides, State of the Art. *ChemCatChem* **2018**, *10*, 4783-4796; (e) Bontemps, S. Boron-Mediated Activation of Carbon Dioxide. *Coord. Chem. Rev.* **2016**, *308*, Part 2, 117-130; (f) Chong, C. C.; Kinjo, R. Catalytic Hydroboration of Carbonyl Derivatives, Imines, and Carbon Dioxide. *ACS Catal.* **2015**, *5*, 3238-3259; (g) Tlili, A.; Blondiaux, E.; Frogneux, X.; Cantat, T. Reductive functionalization of CO<sub>2</sub> with amines: an entry to formamide, formamidine and methylamine derivatives. *Green Chem.* **2015**, *17*, 157-168; (h) Fernandez-Alvarez, F. J.; Aitani, A. M.; Oro, L. A. Homogeneous catalytic reduction of CO<sub>2</sub> with hydrosilanes. *Catal. Sci. Technol.* **2014**, *4*, 611-624; (i) Burkart, M. D.; Hazari, N.; Tway, C. L.; Zeitler, E. L. Opportunities and Challenges for Catalysis in Carbon Dioxide Utilization. *ACS Catal.* **2019**, *9*, 7937-7956.
11. (a) Cramer, H. H.; Chatterjee, B.; Weyhermüller, T.; Werlé, C.; Leitner, W. Controlling the Product Platform of Carbon Dioxide Reduction: Adaptive Catalytic Hydrosilylation of CO<sub>2</sub> Using a Molecular Cobalt(II) Triazine Complex. *Angew. Chem. Int. Ed.* **2020**, *59*, 15674-15681; (b) Luconi, L.; Rossin, A.; Tuci, G.; Gafurov, Z.; Lyubov, D. M.; Trifonov, A. A.; Cicchi, S.; Ba, H.; Pham-Huu, C.; Yakhvarov, D.; Giambastiani, G. Benzoimidazole-Pyridylamido Zirconium and Hafnium Alkyl Complexes as Homogeneous Catalysts for Tandem Carbon Dioxide Hydrosilylation to Methane. *ChemCatChem* **2019**, *11*, 495-510; (c) Rauch, M.; Parkin, G. Zinc and Magnesium Catalysts for the Hydrosilylation of Carbon Dioxide. *J. Am. Chem. Soc.* **2017**, *139*, 18162-18165; (d) Ríos, P.; Rodríguez, A.; López-Serrano, J. Mechanistic Studies on the Selective Reduction of CO<sub>2</sub> to the Aldehyde Level by a Bis(phosphino)boryl (PBP)-Supported Nickel Complex. *ACS Catal.* **2016**, *6*, 5715-5723; (e) Rios, P.; Curado, N.; Lopez-Serrano, J.; Rodriguez, A. Selective reduction of carbon dioxide to bis(silyl)acetal catalyzed by a PBP-supported nickel complex. *Chem. Comm.* **2016**, *52*, 2114-2117; (f) Metsänen, T. T.; Oestreich, M. Temperature-Dependent Chemoselective Hydrosilylation of Carbon Dioxide to Formaldehyde or Methanol Oxidation State. *Organometallics* **2015**, *34*, 543-546; (g) Lu, Z.; Hausmann, H.; Becker, S.; Wegner, H. A. Aromaticity as Stabilizing Element in the Bidentate Activation for the Catalytic Reduction of Carbon Dioxide. *J. Am. Chem. Soc.* **2015**, *137*, 5332-5335; (h) Courtemanche, M.-A.; Legare, M.-A.; Rochette, E.; Fontaine, F.-G. Phosphazenes: efficient organocatalysts for the catalytic hydrosilylation of carbon dioxide. *Chem. Comm.* **2015**, *51*, 6858-6861; (i) LeBlanc, F. A.; Piers, W. E.; Parvez, M. Selective Hydrosilylation of CO<sub>2</sub> to a Bis(silyl)acetal Using an Anilido Bipyridyl-Ligated Organoscandium Catalyst. *Angew. Chem. Int. Ed.* **2014**, *53*, 789-792; (j) Jiang, Y.; Blacque, O.; Fox, T.; Berke, H. Catalytic CO<sub>2</sub> Activation Assisted by Rhenium Hydride/B(C<sub>6</sub>F<sub>5</sub>)<sub>3</sub> Frustrated Lewis Pairs—Metal Hydrides Functioning as FLP Bases. *J. Am. Chem. Soc.* **2013**, *135*, 7751-7760; (k) Park, S.; Bézier, D.; Brookhart, M. An Efficient Iridium Catalyst for Reduction of Carbon Dioxide to Methane with Trialkylsilanes. *J. Am. Chem. Soc.* **2012**, *134*, 11404-11407; (l) Matsuo, T.; Kawaguchi, H. From Carbon Dioxide to Methane: Homogeneous Reduction of Carbon Dioxide with Hydrosilanes Catalyzed by Zirconium–Borane Complexes. *J. Am. Chem. Soc.* **2006**, *128*, 12362-12363.
12. (a) Wang, X.; Chang, K.; Xu, X. Hydroboration of carbon dioxide enabled by molecular zinc dihydrides. *Dalton Trans.* **2020**, *49*, 7324-7327; (b) Li, J.; Daniliuc, C. G.; Kehr, G.; Erker, G. Preparation of the Borane (Fmes)BH<sub>2</sub> and its Utilization in the FLP Reduction of Carbon Monoxide and Carbon Dioxide. *Angew. Chem. Int. Ed.* **2019**, *58*, 6737-6741; (c) Frick, M.; Horn, J.; Wadepohl, H.; Kaifer, E.; Himmel, H. J. Catalyst-Free Hydroboration of CO<sub>2</sub> With a Nucleophilic Diborane(4). *Chem. Eur. J.* **2018**, *24*, 16983-16986; (d) Murphy, L. J.; Hollenhorst, H.; McDonald, R.; Ferguson, M.; Lumsden, M. D.; Turculet, L. Selective Ni-Catalyzed Hydroboration of CO<sub>2</sub> to the Formaldehyde Level Enabled by New PSiP Ligation. *Organometallics* **2017**, *36*, 3709-3720; (e) Aloisi, A.; Berthet, J.-C.; Genre, C.; Thuery, P.; Cantat, T. Complexes of the tripodal phosphine ligands PhSi(XPPH<sub>2</sub>)<sub>3</sub> (X = CH<sub>2</sub>, O): synthesis, structure and catalytic activity in the hydroboration of CO<sub>2</sub>. *Dalton Trans.* **2016**, *45*, 14774-14788; (f) Jin, G.; Werncke, C. G.; Escudié, Y.; Sabo-Etienne, S.; Bontemps, S. Iron-Catalyzed Reduction of CO<sub>2</sub> into Methylene: Formation of C–N, C–O, and C–C Bonds. *J. Am. Chem. Soc.* **2015**, *137*, 9563-9566; (g) Courtemanche, M.-A.; Pulis, A. P.; Rochette, E.; Legare, M.-A.; Stephan, D. W.; Fontaine, F.-G. Intramolecular B/N frustrated Lewis pairs and the hydrogenation of carbon dioxide. *Chem. Comm.* **2015**, *51*, 9797-9800; (h) Wang, T.; Stephan, D. W. Phosphine catalyzed reduction of CO<sub>2</sub> with boranes. *Chem. Comm.* **2014**, *50*, 7007-7010; (i) Das Neves Gomes, C.; Blondiaux, E.; Thuéry, P.; Cantat, T. Metal-Free Reduction of CO<sub>2</sub> with Hydroboranes: Two Efficient Pathways at Play for the Reduction of CO<sub>2</sub> to Methanol. *Chem. Eur. J.* **2014**, *20*, 7098-7106; (j) Cantat, T.; Gomes, C.; Blondiaux, E.; Jacquet, O. Method for preparing oxyborane compounds for subsequent hydrolysis to give methane derivatives. *WO2014162266A1*, 2014; (k) Espinosa, M. R.; Charboneau, D. J.; Garcia de Oliveira, A.; Hazari, N. Controlling

Selectivity in the Hydroboration of Carbon Dioxide to the Formic Acid, Formaldehyde, and Methanol Oxidation Levels. *ACS Catal.* **2018**, *9*, 301-314.

13. (a) Zhao, Y.; Guo, X.; Ding, X.; Zhou, Z.; Li, M.; Feng, N.; Gao, B.; Lu, X.; Liu, Y.; You, J. Reductive CO<sub>2</sub> Fixation via the Selective Formation of C–C Bonds: Bridging Enaminones and Synthesis of 1,4-Dihydropyridines. *Org. Lett.* **2020**, *22*, 8326–8331; (b) Zhu, D.-Y.; Li, W.-D.; Yang, C.; Chen, J.; Xia, J.-B. Transition-Metal-Free Reductive Deoxygenative Olefination with CO<sub>2</sub>. *Org. Lett.* **2018**, *20*, 3282-3285; (c) Zhu, D.-Y.; Fang, L.; Han, H.; Wang, Y.; Xia, J.-B. Reductive CO<sub>2</sub> Fixation via Tandem C–C and C–N Bond Formation: Synthesis of Spiro-indolepyrrolidines. *Org. Lett.* **2017**, *19*, 4259-4262; (d) Frogneux, X.; Blondiaux, E.; Thuéry, P.; Cantat, T. Bridging Amines with CO<sub>2</sub>: Organocatalyzed Reduction of CO<sub>2</sub> to Amins. *ACS Catal.* **2015**, *5*, 3983-3987.

14. (a) Bontemps, S.; Sabo-Etienne, S. Trapping Formaldehyde in the Homogeneous Catalytic Reduction of Carbon Dioxide. *Angew. Chem. Int. Ed.* **2013**, *52*, 10253-10255; (b) Bontemps, S.; Vendier, L.; Sabo-Etienne, S. Borane-Mediated Carbon Dioxide Reduction at Ruthenium: Formation of C1 and C2 Compounds. *Angew. Chem. Int. Ed.* **2012**, *51*, 1671-1674.

15. (a) Desmons, S.; Zhang, D.; Mejia Fajardo, A.; Bontemps, S. Versatile CO<sub>2</sub> Transformations into Complex Products: A One-pot Two-step Strategy. *JoVE* **2019**, e60348; (b) Bontemps, S.; Vendier, L.; Sabo-Etienne, S. Ruthenium-Catalyzed Reduction of Carbon Dioxide to Formaldehyde. *J. Am. Chem. Soc.* **2014**, *136*, 4419-4425.

16. Suh, H.-W.; Guard, L. M.; Hazari, N. Synthesis and reactivity of a masked PSiP pincer supported nickel hydride. *Polyhedron* **2014**, *84*, 37-43.

17. Butlerow, A. C. *R. Acad. Sci., Paris* **1861**, *53*, 145.

18. Delidovich, I. V.; Simonov, A. N.; Taran, O. P.; Parmon, V. N. Catalytic Formation of Monosaccharides: From the Formose Reaction towards Selective Synthesis. *ChemSusChem* **2014**, *7*, 1833-1846.

19. (a) Desmons, S.; Fauré, R.; Bontemps, S. Formaldehyde as a Promising C1 Source: The Instrumental Role of Biocatalysis for Stereocontrolled Reactions. *ACS Catal.* **2019**, *9*, 9575-9588; (b) Siegel, J. B.; Smith, A. L.; Poust, S.; Wargacki, A. J.; Bar-Even, A.; Louw, C.; Shen, B. W.; Eiben, C. B.; Tran, H. M.; Noor, E.; Gallaher, J. L.; Bale, J.; Yoshikuni, Y.; Gelb, M. H.; Keasling, J. D.; Stoddard, B. L.; Lidstrom, M. E.; Baker, D. Computational Protein Design Enables a Novel one-Carbon Assimilation Pathway. *Proc. Natl. Acad. Sci.* **2015**, *112*, 3704-3709; (c) Poust, S.; Piety, J.; Bar-Even, A.; Louw, C.; Baker, D.; Keasling, J. D.; Siegel, J. B. Mechanistic Analysis of an Engineered Enzyme that Catalyzes the Formose Reaction. *ChemBioChem* **2015**, *16*, 1950-1954; (d) Tajima, H.; Inoue, H.; Ito, M. M. A Computational Study on the Mechanism of the Formose Reaction Catalyzed by the Thiazolium Salt. *J. Comput. Chem., Jpn.* **2003**, *2*, 127-134; (e) Henrique Teles, J.; Melder, J.-P.; Ebel, K.; Schneider, R.; Gehrler, E.; Harder, W.; Brode, S.; Enders, D.; Breuer, K.; Raabe, G. The Chemistry of Stable Carbenes. Part 2. Benzoin-type condensations of formaldehyde catalyzed by stable carbenes. *Helv. Chim. Acta* **1996**, *79*, 61-83; (f) Teles, J. H.; Melder, J. P.; Gehrler, E.; Harder, W.; Ebel, K.; Groening, C.; Meyer, R. Preparation of triazolium and tetrazolium salt catalysts for formaldehyde condensation. EP587044A2, 1994; (g) Shigemasa, Y.; Okano, A.; Saimoto, H.; Nakashima, R. The favored formation of dl-glycero-tetralose in the formose reaction. *Carbohydr. Res.* **1987**, *162*, c1-c3; (h) Castells, J.; Geijo, F.; López-Calahorra, F. The “formoin reaction” : A promising entry to carbohydrates from formaldehyde. *Tetrahedron Lett.* **1980**, *21*, 4517-4520.

20. (a) Matsumoto, T.; Yamamoto, H.; Inoue, S. Selective Formation of Triose from Formaldehyde Catalyzed by Thiazolium Salt. *J. Am. Chem. Soc.* **1984**, *106*, 4829-4832; (b) Yoshihiro, S.; Takaaki, U.; Hiroyuki, S. Formose Reactions. XXVIII. Selective Formation of 2,4-Bis(hydroxymethyl)-3-pentulose in N,N-Dimethylformamide–Water Mixed Solvent. *Bull. Chem. Soc. Jpn.* **1990**, *63*, 389-394; (c) Shigemasa, Y.; Ueda, T.; Sashiwa, H.; Saimoto, H. Formose Reactions. XXXI. Synthesis of Dl-2-C-Hydroxymethyl-3-Pentulose from Formaldehyde in N,N-Dimethylformamide-Water Mixed Solvent (I). *J. Carbohydr. Chem.* **1991**, *10*, 593-605; (d) Shigemasa, Y.; Ueda, T.; Sashiwa, H.; Saimoto, H. Formose Reactions. XXXII. Synthesis of Dl-2-C-Hydroxymethyl-3-Pentulose from Formaldehyde in N,N-Dimethylformamide-Water Mixed Solvent (II). *J. Carbohydr. Chem.* **1991**, *10*, 607-618.

21. NHC **2-6** are known to catalyse formose reaction, see ref 18e and 18f.

22. Hollóczki, O. The Mechanism of N-Heterocyclic Carbene Organocatalysis through a Magnifying Glass. *Chem. Eur. J.* **2020**.

23. Siebert, M.; Krennrich, G.; Seibicke, M.; Siegle, A. F.; Trapp, O. Identifying high-performance catalytic conditions for carbon dioxide reduction to dimethoxymethane by multivariate modelling. *Chem. Sci.* **2019**, *10*, 10466-10474

24. (a) Chatterjee, T.; Boutin, E.; Robert, M. Manifesto for the routine use of NMR for the liquid product analysis of aqueous CO<sub>2</sub> reduction: from comprehensive chemical shift data to formaldehyde quantification in water. *Dalton Trans.* **2020**, *49*, 4257-4265; (b) Kua, J.; Galloway, M. M.; Millage, K. D.; Avila, J. E.; De Haan, D. O. Glycolaldehyde Monomer and Oligomer Equilibria in Aqueous Solution: Comparing Computational Chemistry and NMR Data. *J. Phys. Chem. A* **2013**, *117*, 2997-3008; (c) Sørensen, P. E. The Reversible Addition of Water to Glycolaldehyde in

- Aqueous Solution. *Acta Chem. Scand.* **1972**, *26*, 3357–3365; (d) Collins, G. C. S.; George, W. O. Nuclear magnetic resonance spectra of glycolaldehyde. *J. Chem. Soc. B* **1971**, 1352-1355.
25. Faveere, W.; Mihaylov, T.; Pelckmans, M.; Moonen, K.; Gillis-D'Hamers, F.; Bosschaerts, R.; Pierloot, K.; Sels, B. F. Glycolaldehyde as a Bio-Based C2 Platform Chemical: Catalytic Reductive Amination of Vicinal Hydroxyl Aldehydes. *ACS Catal.* **2020**, *10*, 391-404.
26. Candeias, N. R.; Cal, P. M. S. D.; André, V.; Duarte, M. T.; Veiros, L. F.; Gois, P. M. P. Water as the reaction medium for multicomponent reactions based on boronic acids. *Tetrahedron* **2010**, *66*, 2736-2745.
27. Kofoed, J.; Reymond, J.-L.; Darbre, T. Prebiotic carbohydrate synthesis: zinc–proline catalyzes direct aqueous aldol reactions of  $\alpha$ -hydroxy aldehydes and ketones. *Org. Biomol. Chem.* **2005**, *3*, 1850-1855.